Optics Communications 343 (2015) 1–5

Contents lists available at ScienceDirect

Optics Communications

journal homepage: www.elsevier.com/locate/optcom

Studies on subcritical and overcritical density laser ablated TAC foam targets

S. Chaurasia [a,*], P. Leshma [a], C.G. Murali [a], N.G. Borisenko [b], D.S. Munda [a], A. Orekhov [b], A.I. Gromov [b], Yu. A. Merkuliev [b], L.J. Dhareshwar [a]

[a] High Pressure & Synchrotron Radiation Physics Division, Bhabha Atomc Research Centre, Mumbai 400085, India
[b] P. N. Lebedev Physics Institute, Leninsky Pr 53, Moscow, Russia

ARTICLE INFO

Article history:
Received 7 July 2014
Received in revised form
30 December 2014
Accepted 2 January 2015
Available online 5 January 2015

Keywords:
Laser coupling
Low density plastic foam
X-ray emission
Shadowgraphy

ABSTRACT

In this paper, the interaction of high power laser with low density polymer foam with density as low as 2 mg/cm^3, 4 mg/cm^3, 20 mg/cm^3 30 mg/cm^3 and 50 mg/cm^3 targets are investigated and compared with solid polymer targets. An understanding of such interaction is important from fusion research point of view. Low density foam coating of fusion capsule has been proposed in order to smooth in direct drive scheme and also it is being used as efficient x-ray converter in indirect drive scheme. It is observed that about 75–80% of the laser energy is absorbed in the subcritical (with density <4 mg/cm^3) foam targets and the soft x-ray yield in this case is almost two times that measured in the over dense (supper critical) targets. The optical shadowgraphy of the targets shows that the laser coupling in low density foam is associated with a supersonic heat wave while, with increasing density this phenomenon is replaced by subsonic absorption and shock formation. In the case of a 50 mg/cm^3 foams the foil velocity reduced by 35% (i.e. 5×10^6 cm/s), which further reduced to 3.8×10^6 cm/s in case solid polymer targets.

1. Introduction

Ever since the demonstration of first Ruby Laser by Maiman, scientists had been very enthusiastic about the concept of inertial confinement fusion (ICF) as a potential source of energy and its possible role in weapon oriented program as well [1–3]. Lasers are envisaged as tools of energy transport in ICF, either by direct or indirect drive, because of its ability to concentrate large amount of energy into very small targets at very high power flux levels. In direct drive, a capsule containing a mixture of deuterium (D) and tritium (T) is suddenly subjected to conditions of very high temperature and pressure, by irradiating the capsule with a high power laser, whereas x-rays generated by laser are used to drive the implosion in the latter case. In the indirect drive, a Hohlraum, made of high z material enclosing the ICF capsule, emit x-rays to drive the implosion when heated by the incident laser beam. In order to obtain high gain implosions, hydrodynamic instabilities, laser plasma instabilities etc. are needed to be minimized and coupling of laser energy to the target should be maximized. Therefore, even though, direct drive offers the potential for higher-gain implosions than x-ray drive [4,5], many leading laboratories favor the indirect drive, since conditions imposed on laser beam uniformity, ignition target geometry etc. are less stringent than in the direct drive method and also for better conversion efficiency of driver energy to x-ray yield [6]. Young et al., have demonstrated that, laser driven cylindrical Hohlraums of low density walls machined from Ta_2O_5 foams produce higher radiation temperature than those made of the high density walls (100 mg/cm^3 and 4 g/cm^3 respectively) [7]. Smoothing of the laser imprint, by thermal conductivity in a relatively hot, low density outer layer of the target, is one way of attaining improvement in implosion symmetry [8–10]. Implosion symmetry can also be improved by smoothing the laser imprint using multilayered targets made by coating low-density porous matter on a high z material. The National Ignition Facility (NIF) uses targets made of nanoscale materials like high density carbon, very low density copper and gold foams and graded density foams in their ICF experiments. Plastic foams may be used in experiments [11] studying the equation-of-state (EOS) of various materials at extreme pressures. Considering the important role of low density foams, in the design of ICF targets, information about laser–foam interaction and energy transport in foam layered targets is absolutely necessary. In this paper, we report our studies on the interaction of high power laser with low density polymer foam.

* Corresponding author. Fax: +91 22 25505296.
E-mail address: pgshivanand@gmail.com (S. Chaurasia).

http://dx.doi.org/10.1016/j.optcom.2015.01.001
0030-4018/

2. Experimental set up

A 30 J/ 300–800 ps Nd:Glass laser system in BARC was used in the experiment [12]. The laser was focused with an $f/5$ lens into a chamber evacuated to 4×10^{-5} mbar and intensity on the target was of the order of 10^{13}–2×10^{14} W/cm^2. Four calorimeters – E_1, E_2, E_3 and E_4 – were used to measure the energies of incident laser light, forward scattered light over 2π from the targets, SBS back reflected light, and the transmitted laser energy as shown in the experimental set up in Fig. 1. Three x-ray diodes covered with different x-ray filters namely 5 μm Al (spectral range 0.7–1.65 keV), B-10 (spectral range >0.8 keV) and 20 μm Al (spectrum range >4.8 keV) were installed at a distance of 64 cm from target at an angle of 45° from target normal. Two ion collectors were placed at angles of 45° and 55° respectively from target normal. The accelerated foil movement was determined using two frame optical shadowgraphy with spatial and temporal resolutions of 12 μm and 500 ps respectively. The magnification of the shadowgraph was set to ~3.45 using a imaging lens [13]. The accelerated foil movements were recorded for two optical delays 4.82, and 8.29 ns with respect to the arrival of main laser pulse at target. The shadowgrams of TAC (Triacetate cellulose) target foils of thickness 100 ± 20 μm with density 2 mg/cm^3, 4 mg/cm^3, 20 mg/cm^3, 30 mg/cm^3, and 50 mg/cm^3 at optical delay of 4.82 ns are shown in Fig. 5a–e. The shadowgram of 15 μm thick polymer of density 1.26 g/cm^3 at optical delay of 4.82 ns is shown in Fig. 5f. In all cases the laser energy on target was 7.5 ± 0.2 J. Targets used in these experiments were low density foam targets. The material used was cellulose triacetate (TAC – $C_{12}H_{16}O_8$). The structure realized was typical of an aerogel, and looked like a 3D-network with sub-micron fibers. A 10 mg/cm^3, Tri Acetate Cellulose (TAC) target mounted on the copper washer is shown in Fig. 2a and the SEM record is shown in Fig. 2b.

3. Result and discussion

The x-ray intensity from the laser produced plasma depends on parameters such as laser intensity, pulse duration and laser to x-ray conversion efficiency. The x-ray conversion efficiency was optimized by changing the density of the foam targets keeping the thickness same. The x-ray signal recorded with the x-ray diodes for soft and hard x-rays are shown in Fig. 3a and b, and Fig. 4 respectively. From Fig. 3a and b, it is clear that, for soft x-ray yield, there are two distinct regions: region of slowly varying x-ray conversion efficiency (corresponding to higher density) and that of significantly fast changing x-ray conversion efficiency corresponding to lower density. The x-ray emission conversion efficiency in the x-ray spectral range (0.8–1.56 keV) increases slowly by 25% for the solid density (1.26 g/cm^3 to 30 mg/cm^3) and then increases fast (by 50%) for 30–2 mg/cm^3. Similarly, for the x-ray spectral range >0.9 keV, it was observed that, conversion efficiency initially increases, by 10% when density is varied from solid density to 30 mg/cm^3 and then by 50% for variation from 30 mg/cm^3 to 2 mg/cm^3. Fig. 4 shows the variation of hard x-ray yield with target density in the spectral range 4–16.4 keV. In this case, the hard x-ray yield was 700% from solid density to 30 mg/cm^3 and 50% from 30 g/cm^3 to 2 mg/cm^3. In the density range from 50 mg/cm^3 to 2 mg/cm^3, the trend for hard x-rays is same as for soft x-rays emission, however, for the density >50 mg/cm^3, the hard x-rays emission further decreases compared to soft x-ray yield which is almost constant for the density >50 mg/cm^3. The reason for the x-ray enhancement can be explained as follows. In the case of under-dense foam target, where electron densities are lower than the critical density, (only at density <4 mg/cm^3, the plasma is actually under-dense), the laser energy is directly absorbed at the x-ray emission region via inverse bremsstrahlung for that particular drive laser wavelength. Due to the larger density gradient scale length, and heating, which is volumetric and highly supersonic without any hydrodynamic energy losses, the x-ray generation becomes efficient and enhanced. The fractional absorption of the laser can be written as $A_L \approx 1 - \exp\left[-0.007Z'L/\left(\lambda^2 T_e^{3/2}\right)\right]$ [14],where Z' is the average degree of ionization, L is the density gradient length, λ is the wavelength, and T_e is the electron temperature. In target with larger density, the plasma is over dense (supercritical), the density gradient and temperature gradient scale length decrease and the laser energy absorbed at critical density is transported via electron thermal conduction into the dense region. Hence, the x-ray emission region for the high dense targets is reduced due to steep gradients in density and temperature in plasma. The steepening of the plasma density and temperature increase, corresponding to the increase in density, reduce the heated volume. The same can be seen from the shadowgraphs shown in Fig. 5a–f recorded for targets with density 2 mg/cm^3, 4 mg/cm^3, 20 mg/cm^3, 30 mg/cm^3, 50 mg/cm^3 and solid polymer of density 1.26 g/c. The plasma volume reduces with increasing target density. From these figures it can also be noted that the lateral plasma dimension decreases with density. The scaling of the lateral foil expansion and foil

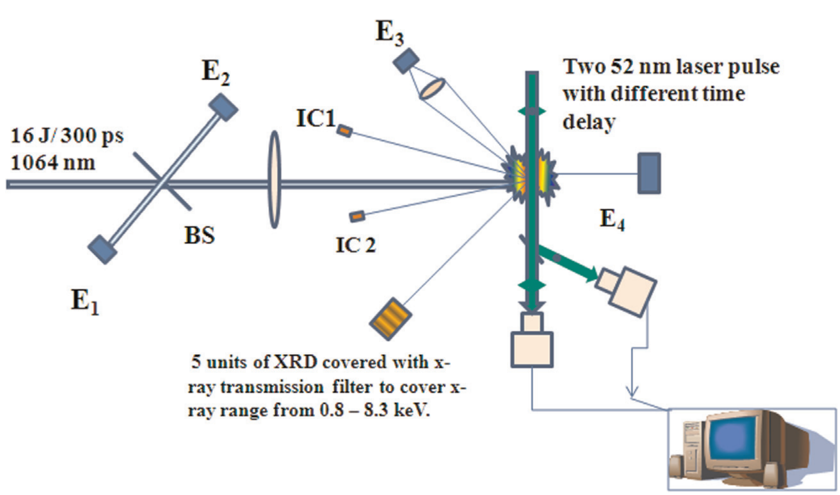

Fig. 1. Experimental set up. Four energy meters E_1, E_2, E_3 and E4 are used for energy balance measurement. Ion collectors IC_1 and IC_2 are used for ion signal detections. An unit of five x-ray diodes are used for x-ray spectrum recording. Two CCD cameras were used for simultaneous recording of two shadowgrams of different time delays.